

# **Supplementary Information to: "Storm Boris (2024) in the current and future climate: a dynamics-centered contextualization, and some lessons learnt"**

Jacopo Riboldi<sup>1,\*</sup>, Robin Noyelle<sup>1,\*</sup>, Ellina Agayar<sup>1</sup>, Hanin Binder<sup>1</sup>, Marc Federer<sup>1</sup>, Katharina Hartmuth<sup>1</sup>, Michael Sprenger<sup>1</sup>, Iris Thurnherr<sup>1</sup>, and Selvakumar Vishnupriya<sup>1</sup>

<sup>1</sup>Institute for Atmospheric and Climate Science, ETH Zurich, Zurich, Switzerland

*\*These authors contributed equally to this work*

**Correspondence:** jacopo.riboldi@env.ethz.ch

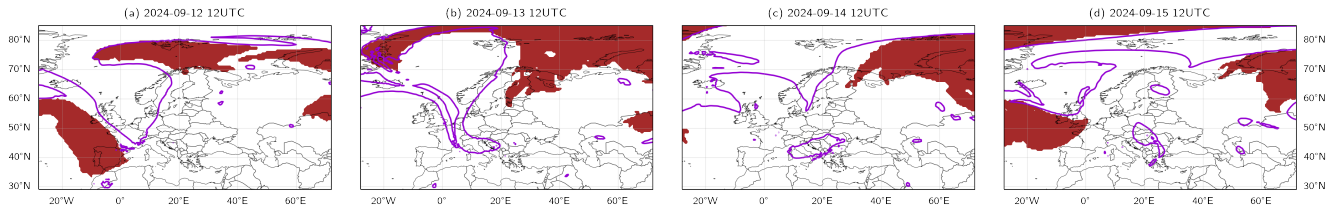


**Figure S1.** Atmospheric blocking events (in red) during Storm Boris, identified in the ECMWF analysis using the Schwierz et al. (2004) method with a  $-0.7$  PVU anomaly threshold, along with 2 PVU at 320 K (purple contour).

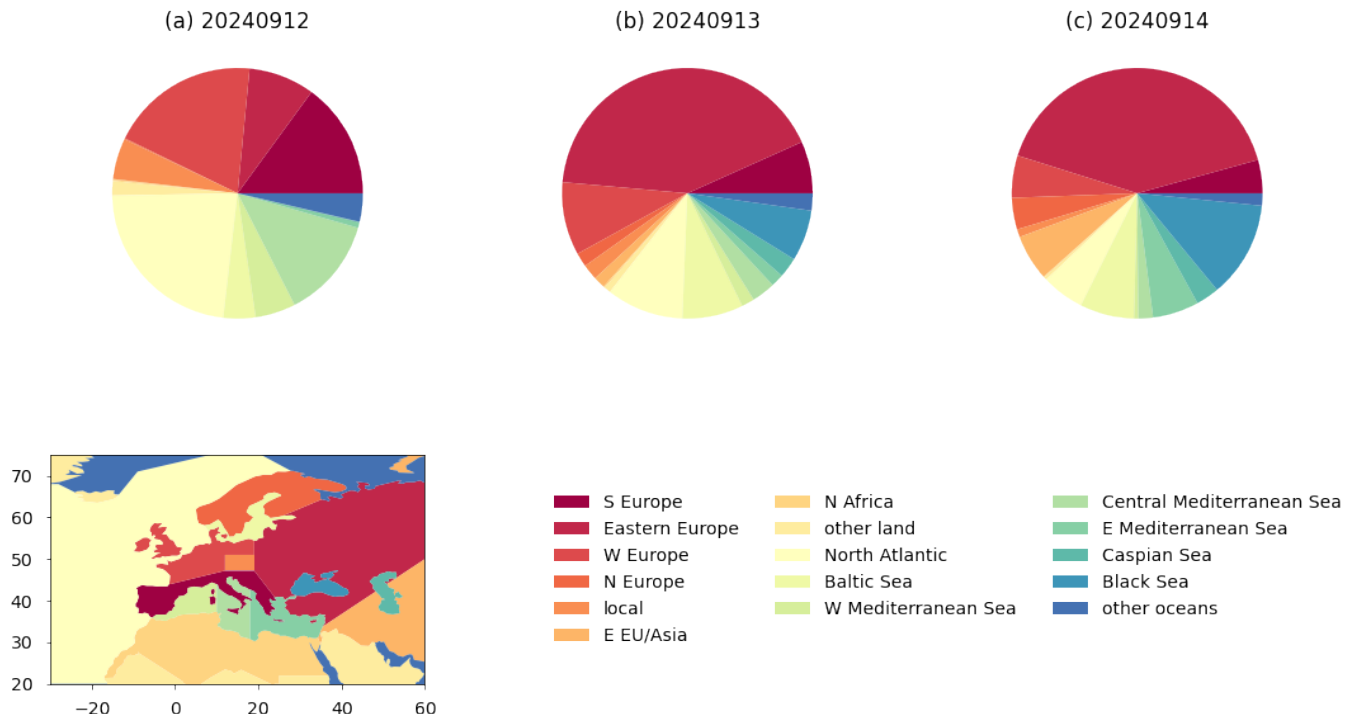
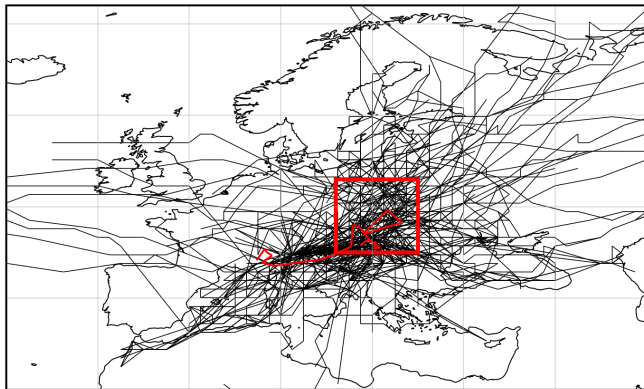
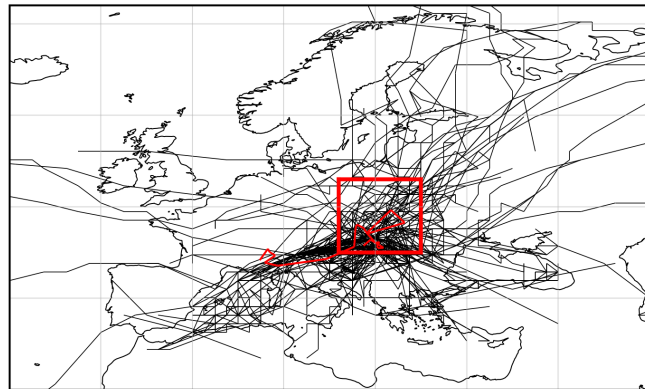


**Figure S2.** (Top) Relative moisture source contributions [%] from subregions (colors) for precipitation in the target region ("local") on (a) 12, (b) 13, and (c) 14 Sep 2025. (Bottom) Map overview of defined subregions.

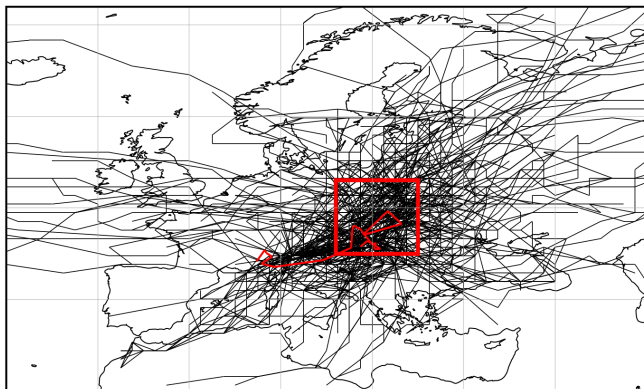
a Seasonal PV analogs (1990-1999)



b Seasonal PV analogs (2091-2100)



c Yearly PV analogs (1990-1999)



d Yearly PV analogs (2091-2100)

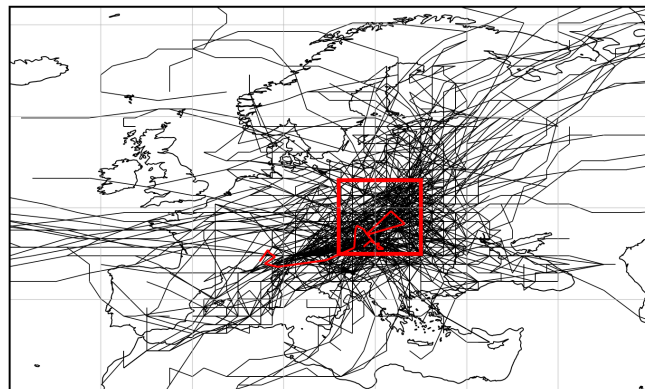


**Figure S3.** Tracks of selected cyclones for the (a,b) seasonal and (c,d) yearly PV analogs in the CESM1 simulation in the periods (a,c) 1990–1999 and (b,d) 2091–2100. All tracks must be located within the red box at the analog time step. The red track indicates the track of storm Boris.

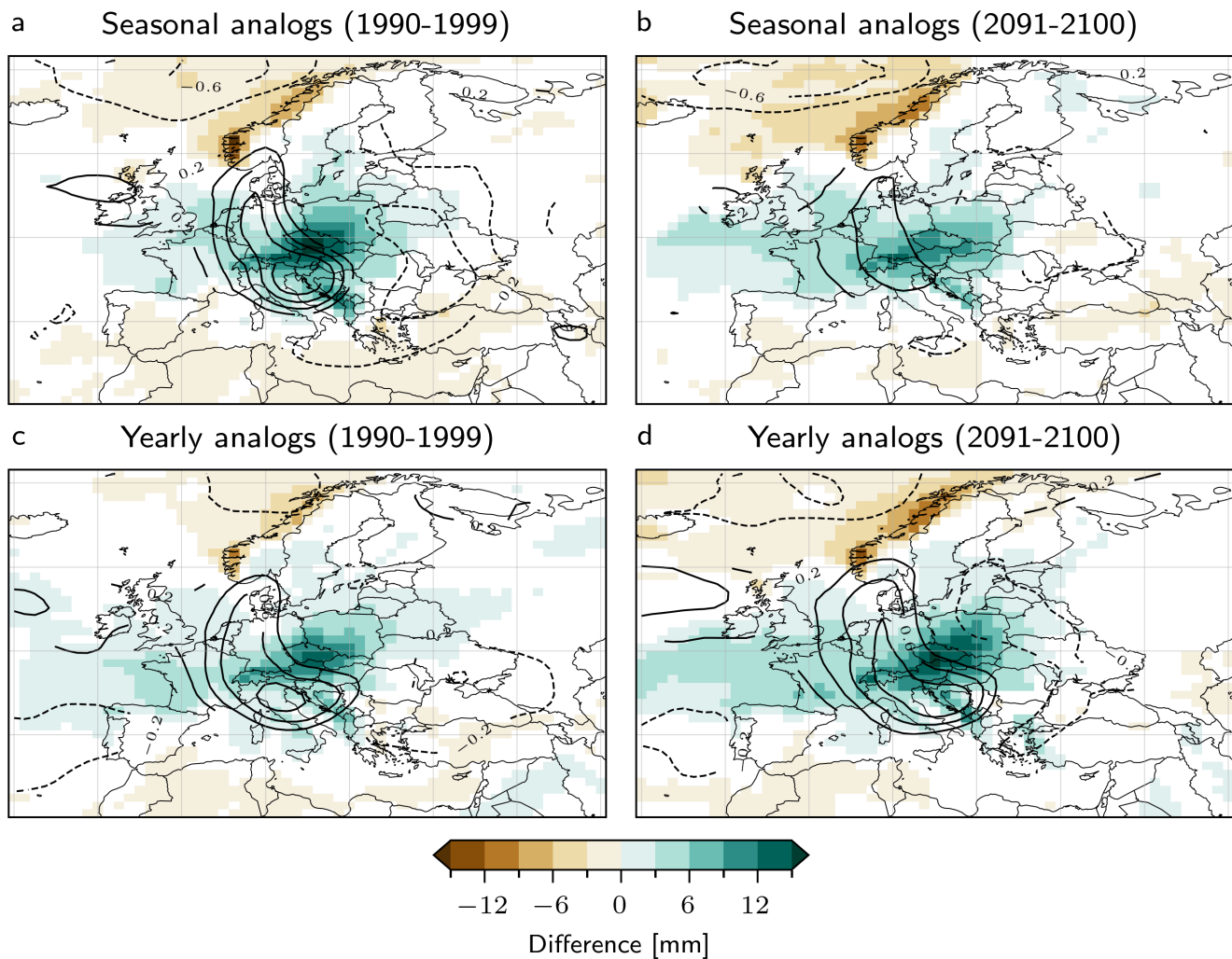


**Figure S4.** Difference of mean 5-day cumulated precipitation (colors) and 250 hPa PV (contours) between selected and non-selected analogs for the (a,b) seasonal and (d,e) yearly PV analogs in the periods (a,d) 1990–1999 and (b,e) 2091–2100. Grid points with no significant differences (see text) are marked as white for the precipitation field and not shown for the PV field. The PV contours are drawn every 0.2 PVU.



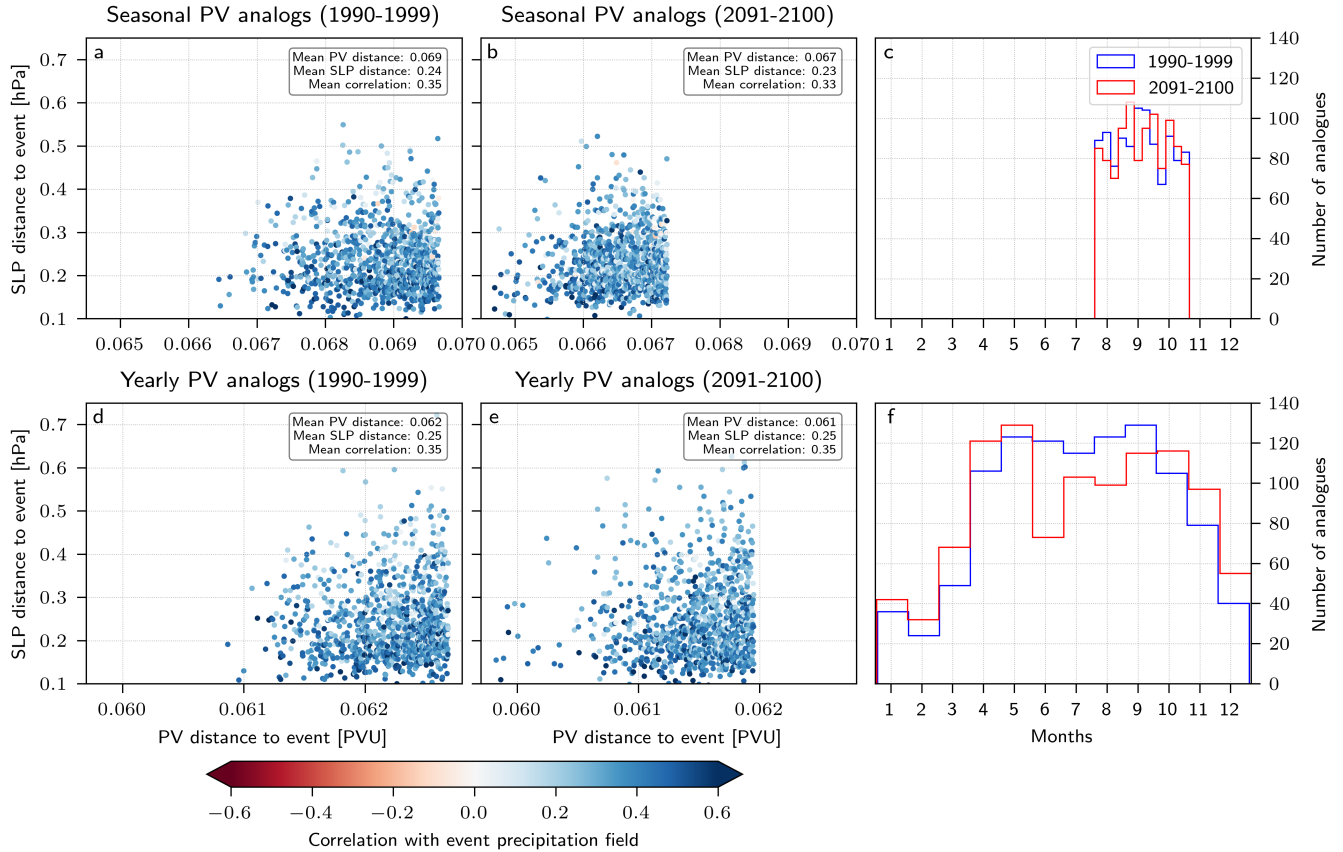


**Figure S5.** Distances between the analogs and the event fields and dates distribution of the analogs. Mean distance to the PV field of the event (x-axis) and the SLP field of the event (y-axis) for the  $n = 1050$  (a,b) seasonal and (d,e) yearly PV analogs in the CESM1 simulation in the periods (a,d) 1990–1999 and (b,e) 2091-2100. Colors show the Spearman spatial correlation between the precipitation fields of the analogs and the event. All metrics are computed using the fields over the region where the analogs are computed (32°N-70°N, 5°W-40°E). Distributions of the day-of-year dates of the (c) seasonal and (d) yearly analogs.

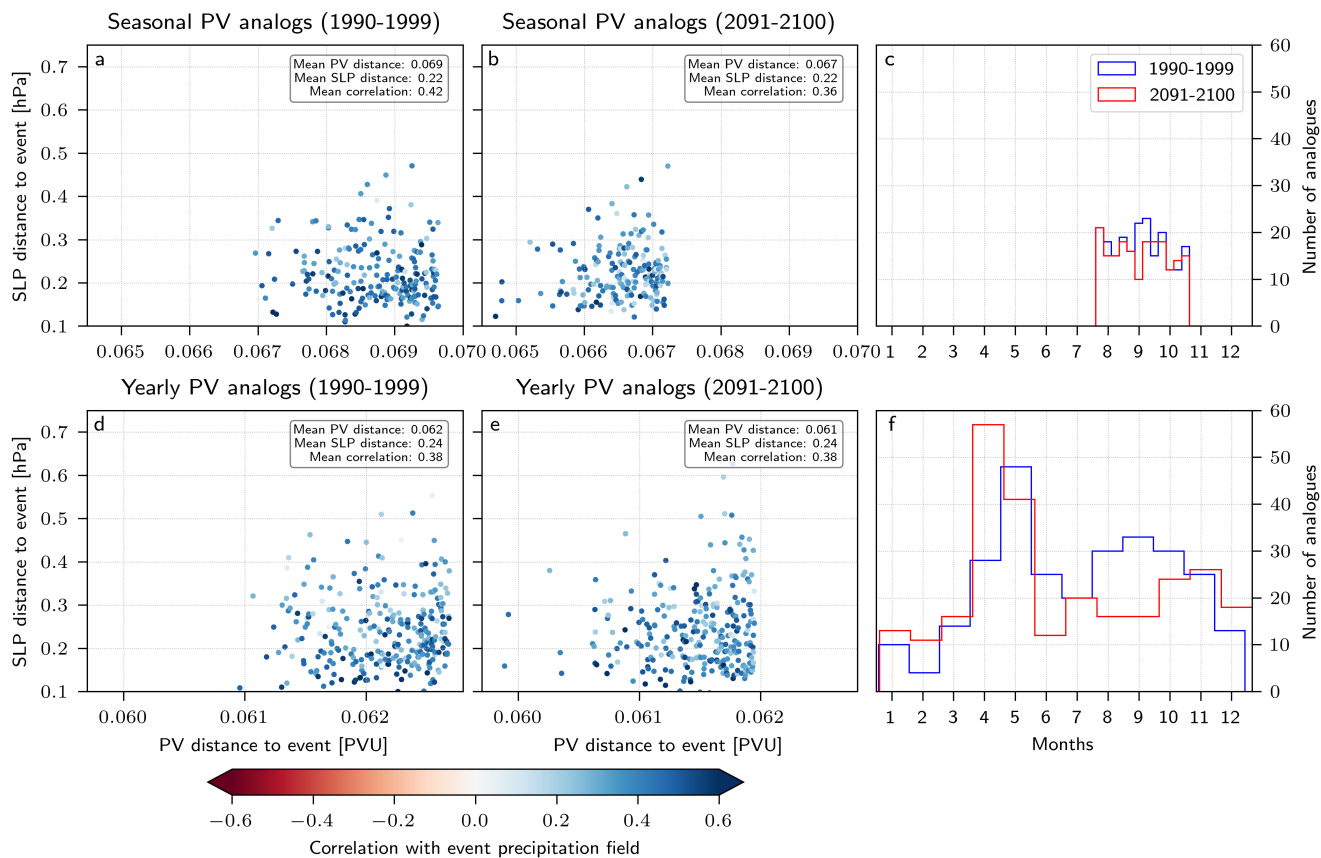


**Figure S6.** Same as Figure S5 but for analogs with a low-level cyclone. (a)  $n = 210$ , (b)  $n = 190$ , (d)  $n = 280$ , (e)  $n = 270$ .

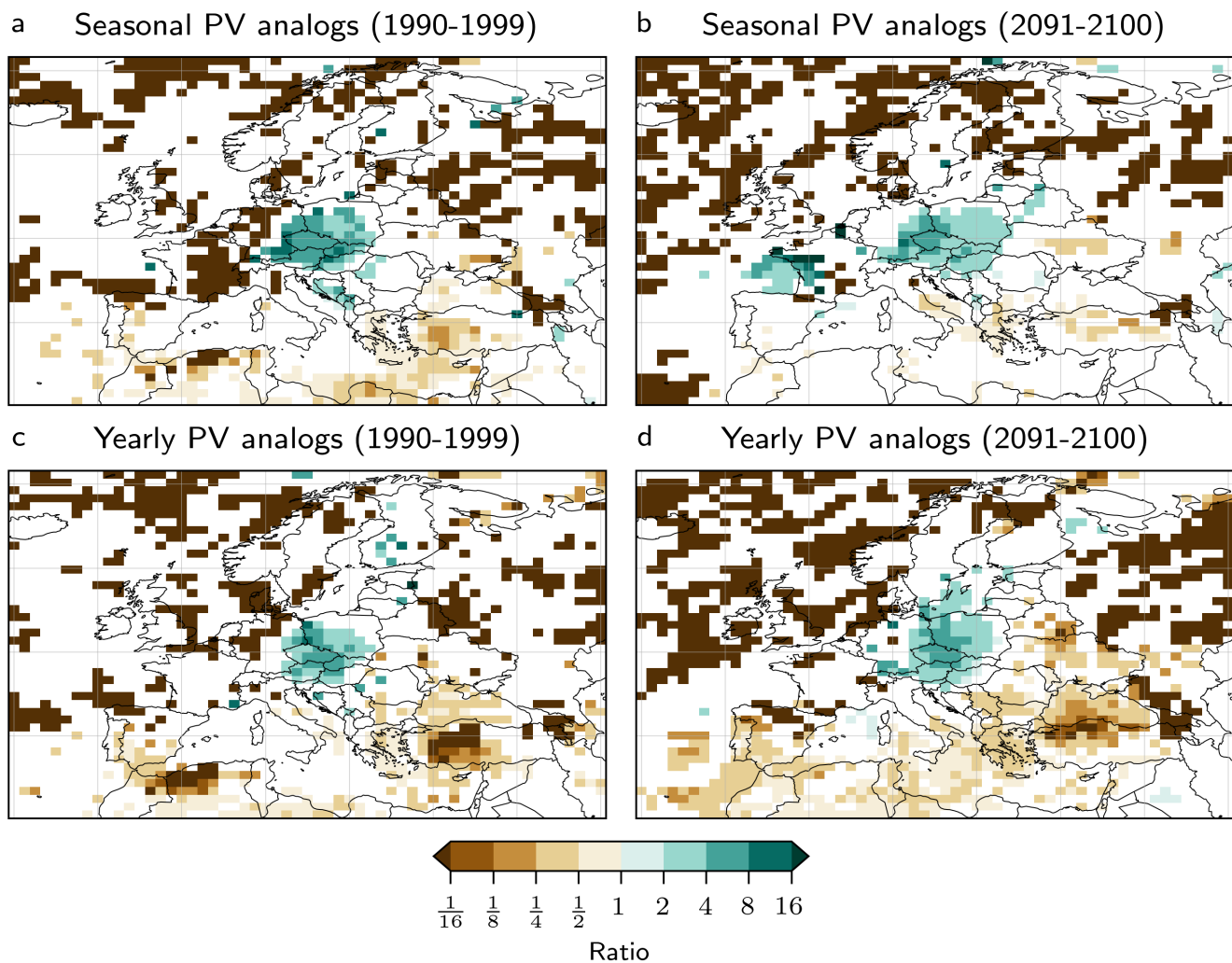


**Figure S7.** Ratio of the frequencies of analogues reaching the 75th climatological quantile of 5-day cumulated precipitation (colors) and 250 hPa PV (contours) between selected and non-selected analogs for the (a,b) seasonal and (d,e) yearly PV analogs in the periods (a,d) 1990–1999 and (b,e) 2091–2100. Grid points with no significant differences (assessed as detailed in Sect. 2.2) are marked as white for the precipitation field and not shown for the PV field. The PV contours are drawn every 0.2 PVU.

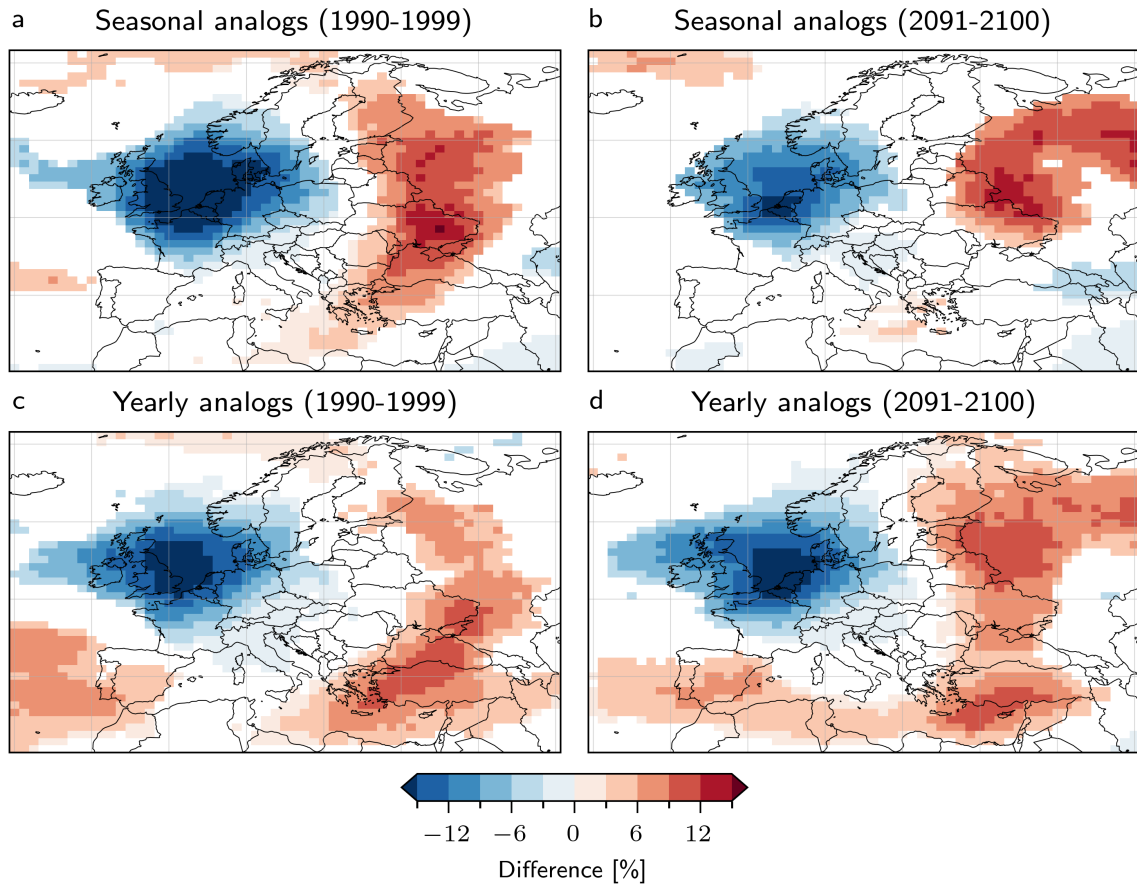


**Figure S8.** Difference in blocking frequency (shaded) between selected and non-selected analogs for the (a,b) seasonal and (c,d) yearly PV analogs in the periods (a,c) 1990–1999 and (b,d) 2091–2100. Grid points with no significant differences (assessed as detailed in Sect. 2.2) are marked in white.

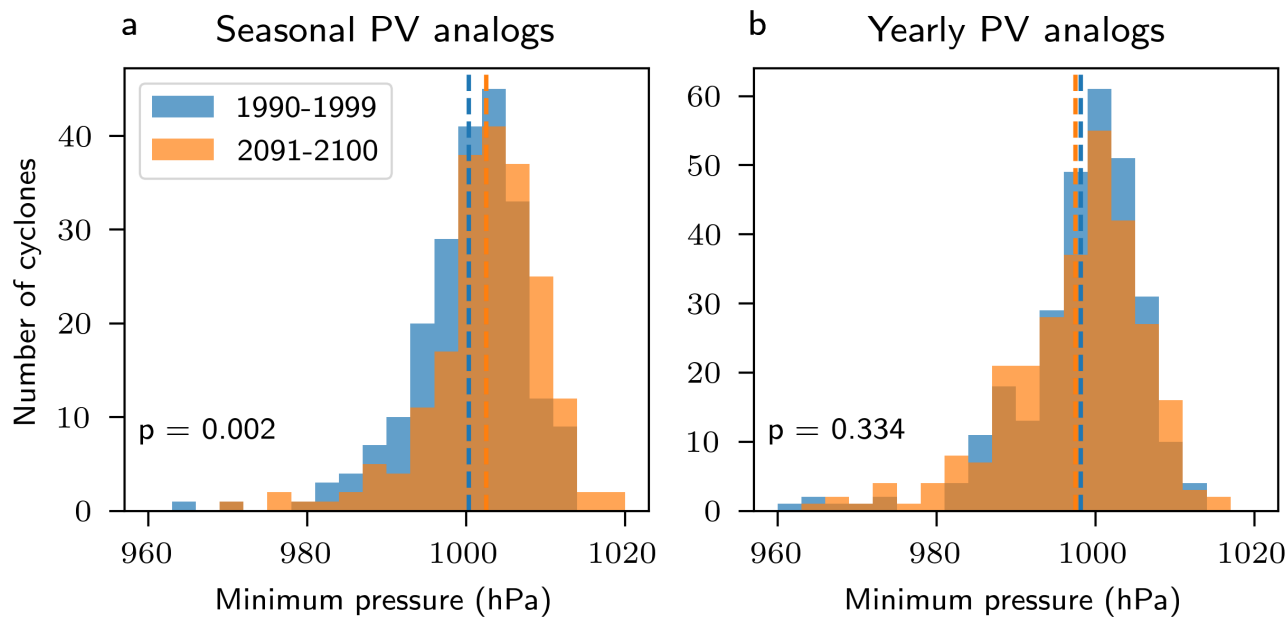


**Figure S9.** Histograms of the minimum SLP along selected cyclone tracks in the CESM1 simulation for the (a) seasonal and (b) yearly PV analogs. Results are shown for the historical period (1990–1999, blue) and the future period (2091–2100, orange). Dashed vertical lines indicate the mean minimum SLP for each period. The p-values from a two-sample t-test assess the statistical significance of differences in the mean values.

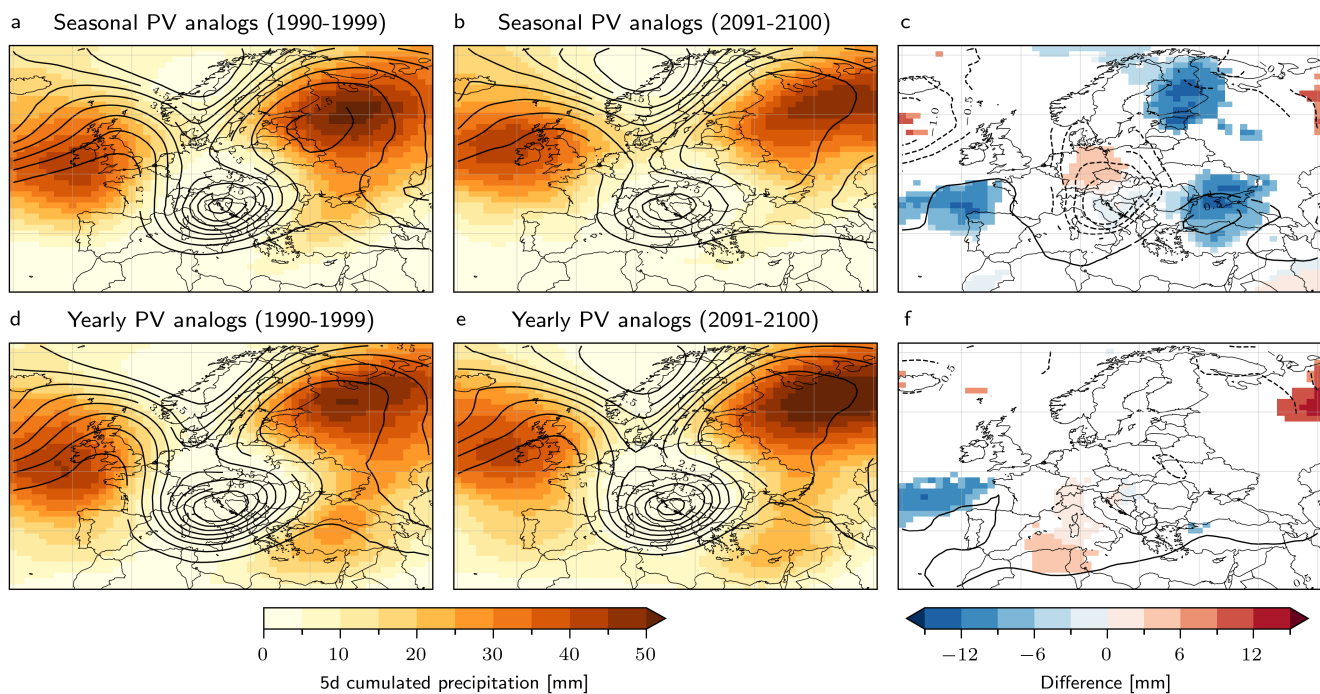


**Figure S10.** As Figure 6, for the frequencies of blocking at each grid point.

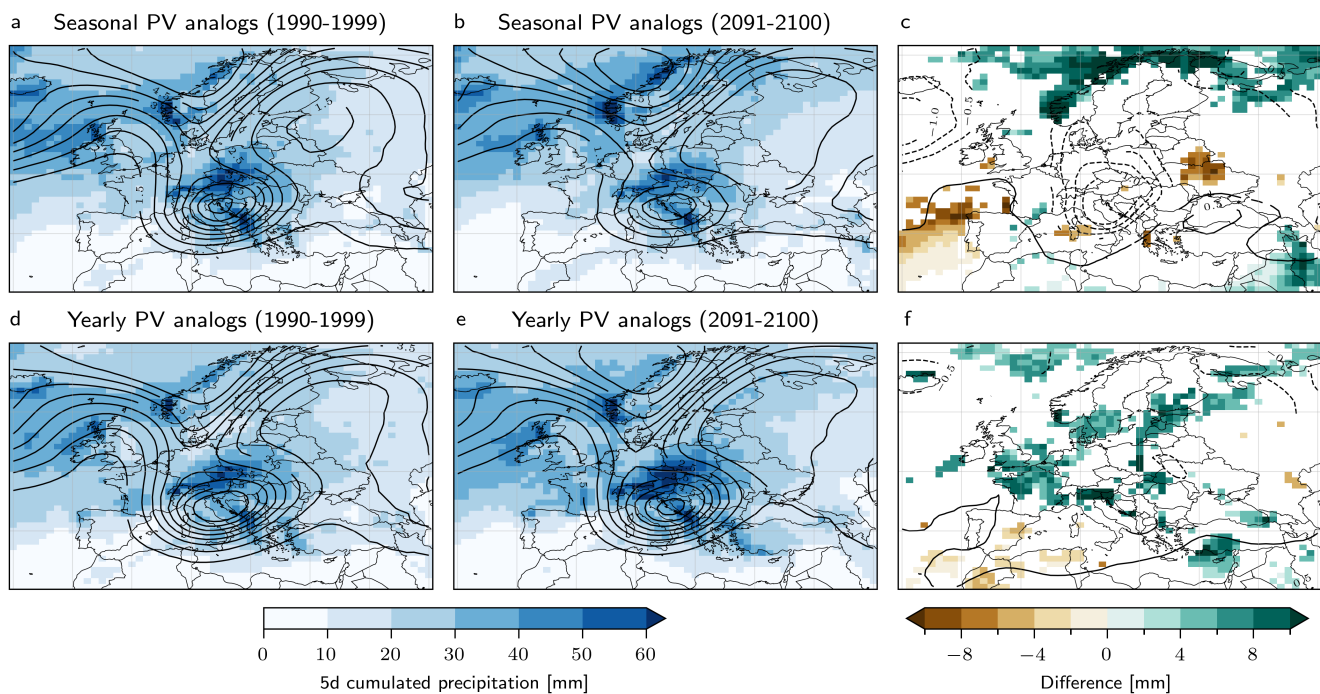


**Figure S11.** Same as Figure 6 using the 90th quantile of the analogs distribution for the precipitation field.



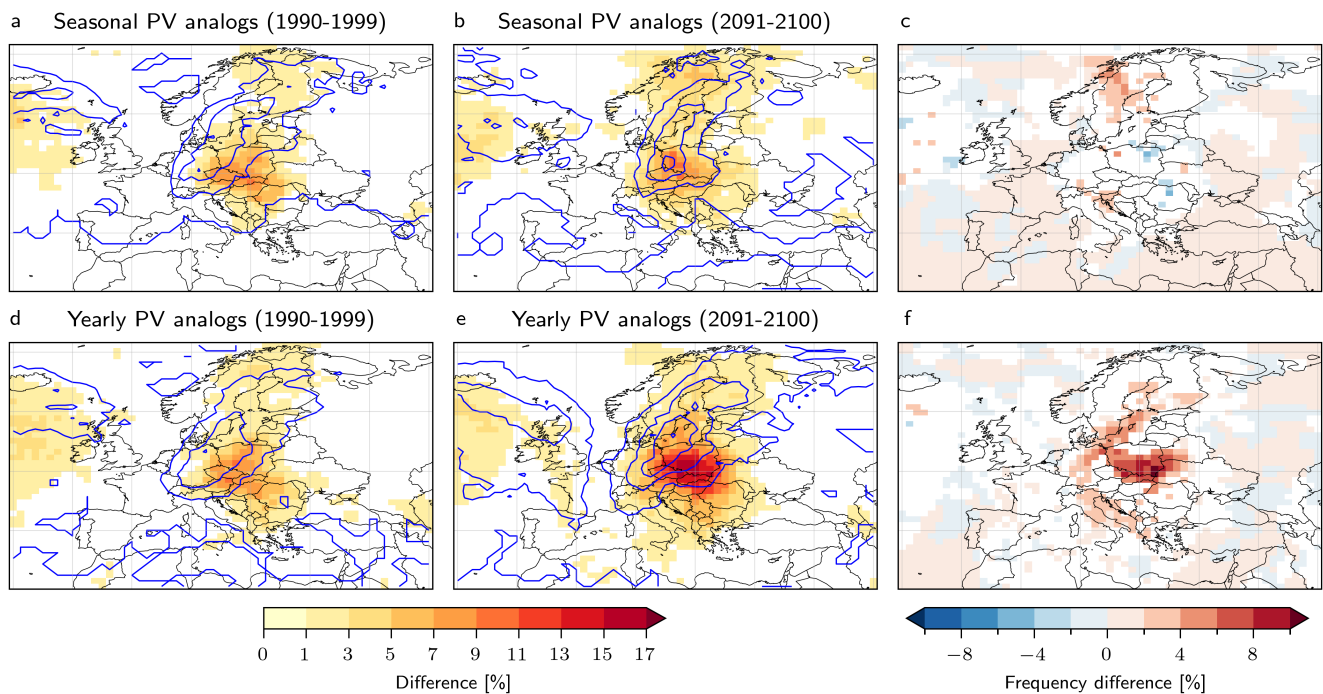


**Figure S12.** As Figure 6, displaying for the frequencies of gridded WCB ascent (shaded,  $400 < p < 800$  hPa) and outflow (blue contours,  $p < 400$  hPa) trajectories at each grid point. Definition of WCB ascent and outflow masks and of the gridding procedure are explained in detail in Heitmann et al. (2024).

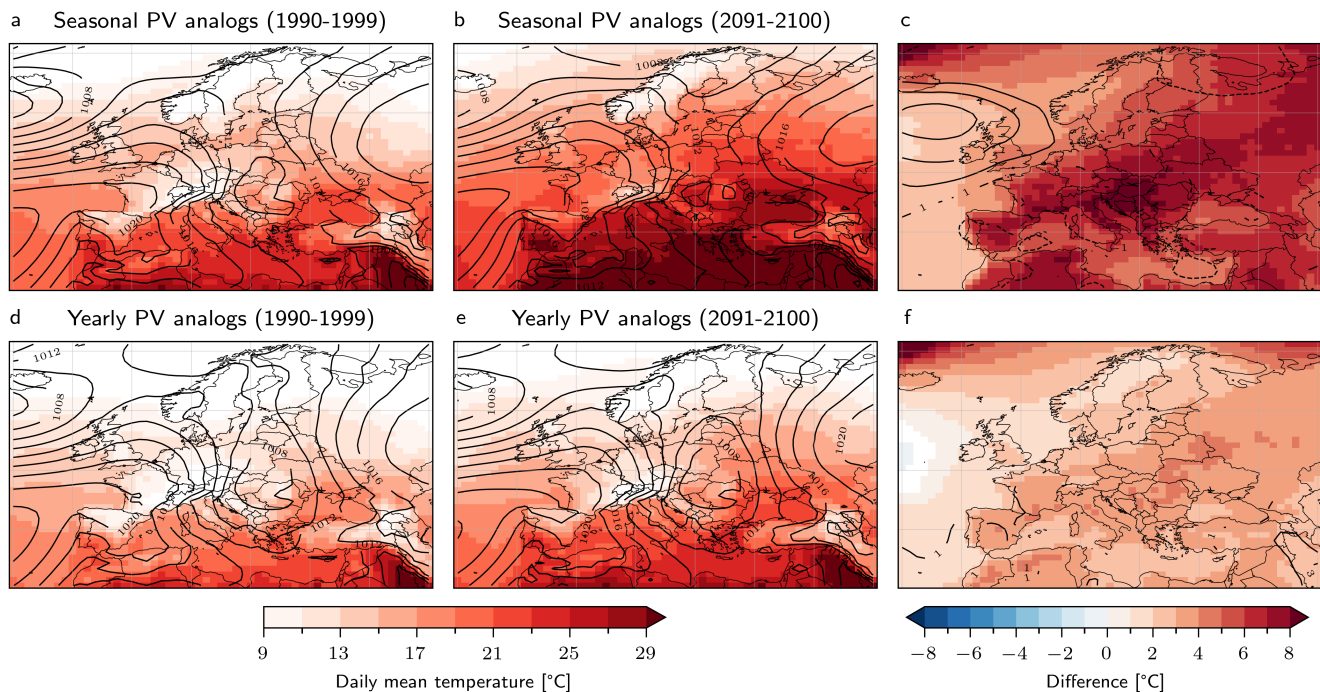


**Figure S13.** Change in the mean temperature and SLP fields of the analogs between the two periods. Mean 2-m air temperature (colors) and SLP (contours) for the (a,b) seasonal and (d,e) yearly PV analogs in the periods (a,d) 1990–1999 and (b,e) 2091–2100. The SLP contours are drawn every 2 hPa. Difference between the two periods for (c) seasonal and (f) yearly analogs. Grid points with no significant differences (see text) are marked as white for the temperature field and not shown for the SLP field.

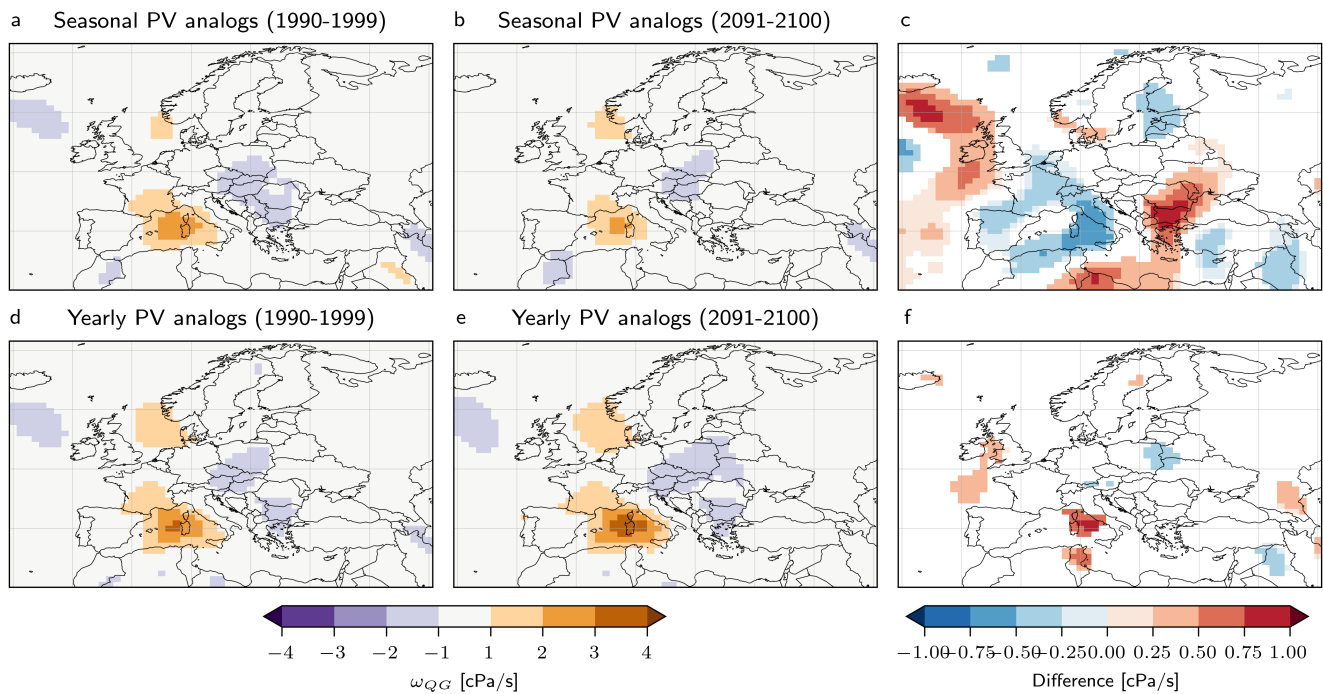


**Figure S14.** Same as Figure 9 for the forcing at 650hPa due to lower levels.

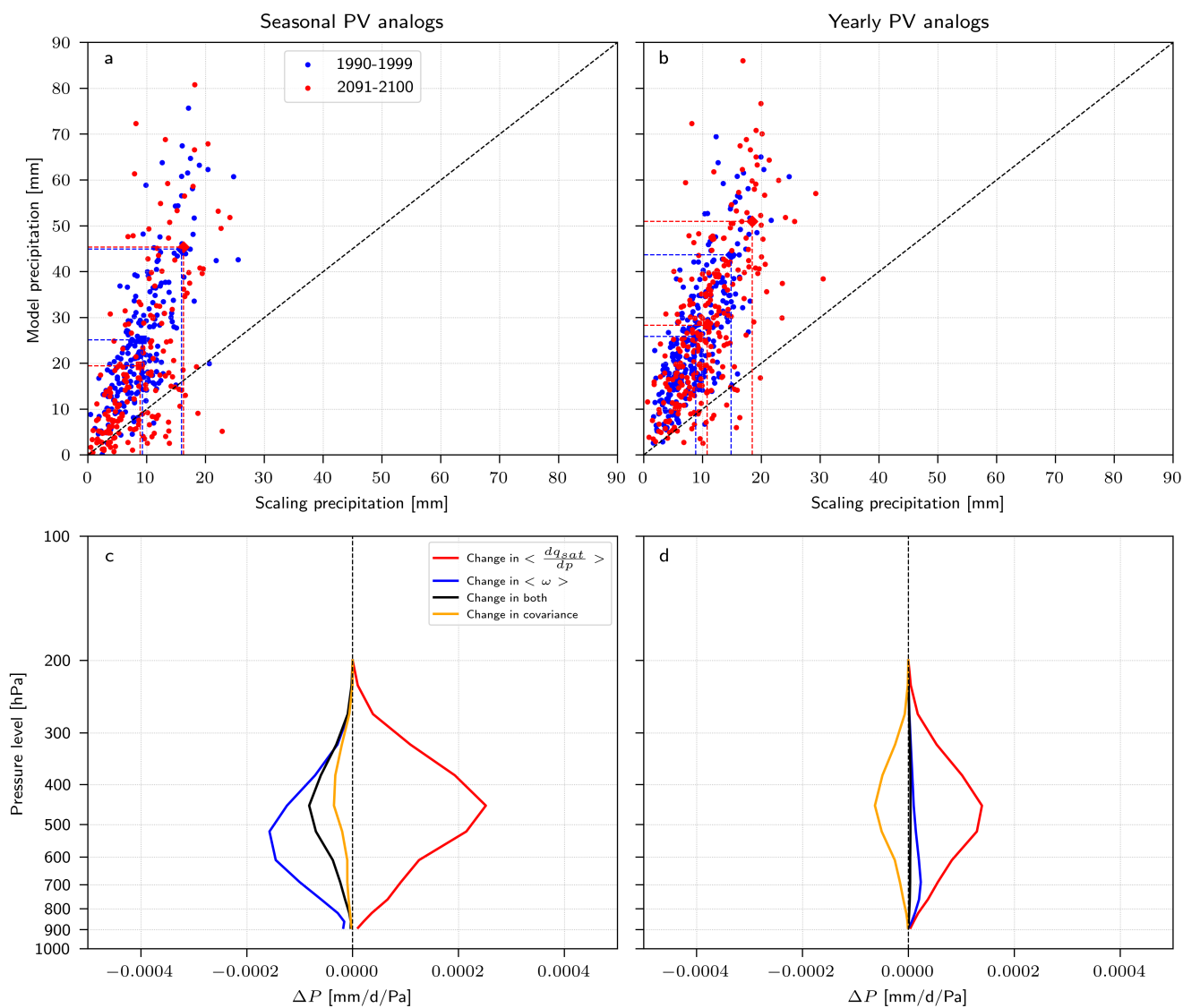


**Figure S15.** Same as Figure 8, using the QG vertical wind speed in the scaling equation.

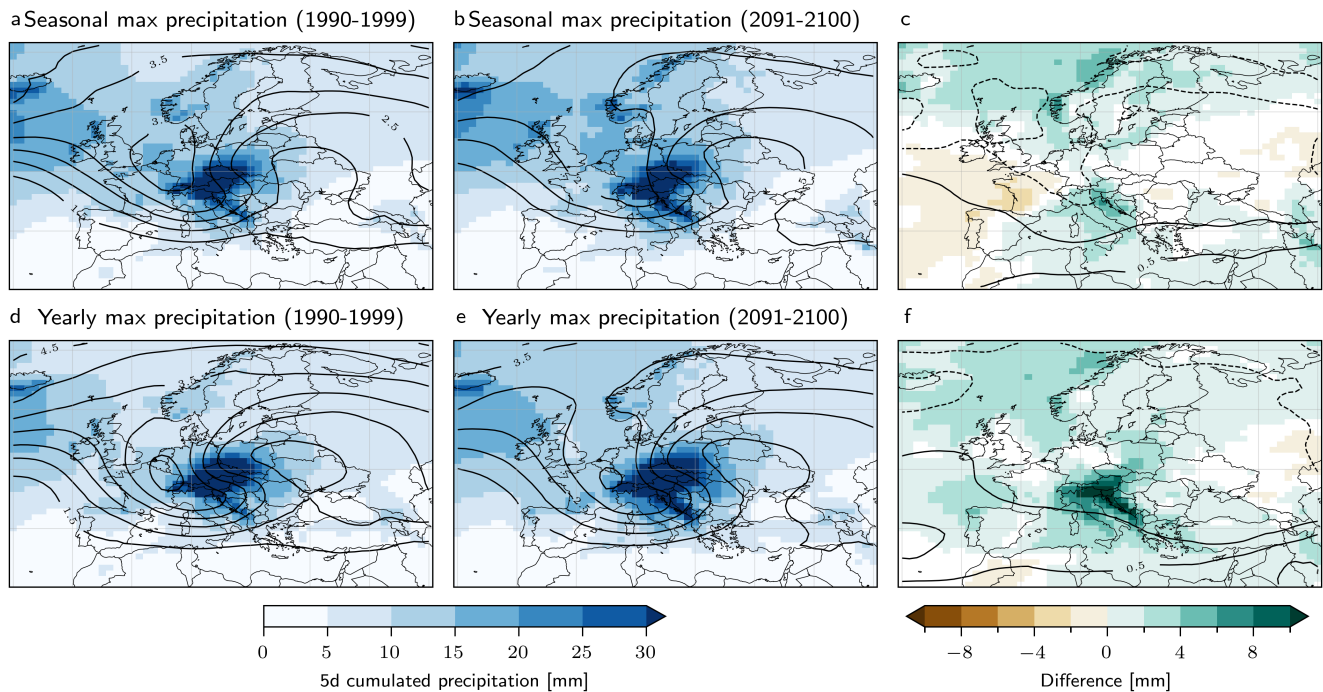


**Figure S16.** Same as Figure 6 for the (a,b) seasonal and (d,e) yearly maximum 5-day cumulated precipitation events. There are  $n = 1050$  events averaged in each panel.